



WALLACE H. COULTER SCHOOL OF ENGINEERING
Technology Serving Humanity

MEMORANDUM

From: Bill Jemison
To: Dr. Daniel Tam, ONR
Date: 8/29/2011

Subject: Progress Report 004—
Chaotic LIDAR for Naval Applications: FY11 Progress Report (7/11/2010– 8/29/2011)

This document provides a progress report on the project "Chaotic LIDAR for Naval Applications" covering the period of FY11 (7/1/2010–8/29/2011).

20150309444

FY11 Progress Report: Chaotic LIDAR for Naval Applications

This document contains a **Progress Summary for FY11** and a **Short Work Statement for FY12**.

Progress Summary for FY11

The original proposal identified the following three tasks:

- Task 1 involves the generation and characterization of a wideband CLIDAR signal suitable for system-level experiments. Our proposed approach uses a continuous wave (CW) laser to excite non-paraxial propagation in an open optical resonator (OOR).
- Task 2 involves a system-level investigation into the underwater propagation/scattering characteristics of the CLIDAR signals. The investigation will be performed as a function of both optical wavelength and water turbidity (absorption and scattering) in order to determine the range resolution/accuracy and signal to noise performance that can be expected using CLIDAR.
- Task 3 involves the development of an advanced chaotic laser, or CLASER, for use as a compact and cost-effective optical source for CLIDAR. This approach integrates a laser gain medium into an OOR to produce an integrated chaotic optical source.

Task 1 - Task 1 efforts were pursued early in the program and focused on the feasibility of using the open optical resonator (OOR) approach to produce wideband chaotic laser signals. The task was identified as a precursor to the more important Task 3. OORs can theoretically support many simultaneous longitudinal modes necessary for wideband chaotic signal generation. We developed a simulation to allow us to design OORs to support high order modes such as the "M" mode shown in Figure 1 as a first step to the chaotic OOR. The simulation allowed us to determine the excitation conditions (e.g. the angle and lateral offset necessary for a given mode with a specified set of mirrors and cavity length). For example, the "M" mode is a stable mode that traces a path in the resonator that includes two distinct reflection points on one of the resonator mirrors and three distinct reflection points on the other resonator mirror. The upper plot in Figure 1 shows the ray trajectory of a cavity designed for the "M" mode. The photograph shown in Figure 1 shows the two reflection points on the left resonator mirror.

Our initial experimental work convinced us that there are two drawbacks to this approach. The first is that custom optics are required to minimize coupling losses into and out of the resonator. We were not able to find commercial off-the-shelf (COTS) components for the OORs that we wished to design. High coupling losses would preclude the generation of high optical power levels necessary for system-level experiments. Second, the OORs require precise positioning accuracies and would necessitate the use of expensive kinematic positioners and optical tables which are also not desirable for the system-level experiments that are planned.

Therefore, we decided to abandon the Task 1 OOR approach and proceed directly to Task 3 and the development of a laser that would produce the desired wideband signals. Task 3 will be discussed next followed by our Task 2 efforts.

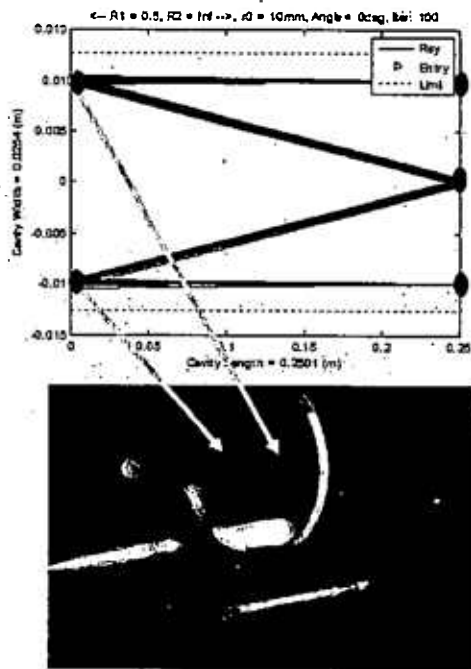


Figure 1. Initial experiments on Open Optical Resonators. Generation of a stable higher order “M” mode is shown. This approach was abandoned due to the complexity and lack of COTS components.

Task 3 – Based on our investigations into OORs, we reexamined other approaches for wideband optical generation. We selected a fiber laser approach is extremely promising. Fiber lasers are a mature technology and commercially available products are available at 532nm as well as in the 1100-1700 nm range. Output powers are available in the 0.5W to 30W range which are compatible with system-level experiments. Further, experimental fiber lasers are relatively easy to build. Several companies sell doped fiber and at least two companies offer fiber laser simulation software. The fiber laser configuration that we selected is a ring configuration with a long resonator cavity that will support many simultaneous longitudinal lasing modes necessary for wideband signal generation. These fiber ring laser longitudinal modes are much easier to obtain than those of the OOR since they may be generated by simply using a long piece (~km) of optical fiber excited by normal fiber optical coupling. The OOR, on the other hand, required precise input and output free space coupling conditions.

Two fiber ring lasers have been developed to date. The first, operating at 1550 nm, was presented at a project review held at NAWC, Patuxent River, MD on August 3rd. The second, operating at 1071 nm has been developed since then. Each will be briefly described. Both are based on the ring laser configuration shown below in Figure 2.

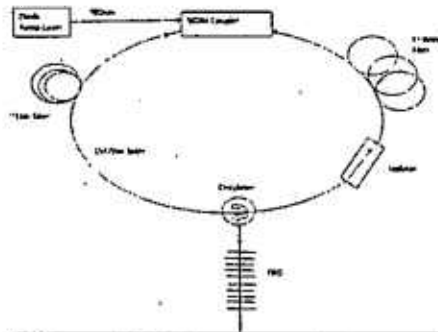


Figure 2. Fiber ring laser geometry used for both the 1550 and 1071 nm lasers. Specific components are shown for the 1150 nm laser

1550 nm Fiber Ring Laser - A proof-of-concept fiber ring laser that was constructed using existing components at a wavelength of approximately 1546 nm. This wavelength was selected based on the availability of all necessary fiber laser components. The gain medium is an erbium (Er) doped fiber and this laser is capable of lasing in multiple modes simultaneously. The temporal output is noise-like with a well-defined autocorrelation peak. While we are not pursuing a frequency doubled 1546 nm laser (since we don't believe the wavelength (773 nm) is appropriate for underwater work), we will continue working with this laser to help us explore autocorrelation-based signal processing approaches (described in more detail below). Figures 3 and 4 show additional characterization of the fiber ring laser. Figure 3 shows the optical spectrum of the fiber ring laser. As desired, the laser output consists of many lasing modes occurring over a 1 nm bandwidth defined by the fiber Bragg grating used in the laser cavity. This results in a broadband RF signal upon photo-detection as shown in Figure 4. This RF spectrum has a very flat frequency response from 200 MHz to 4.4 GHz (which is the limitation of the existing measurement equipment) as desired.

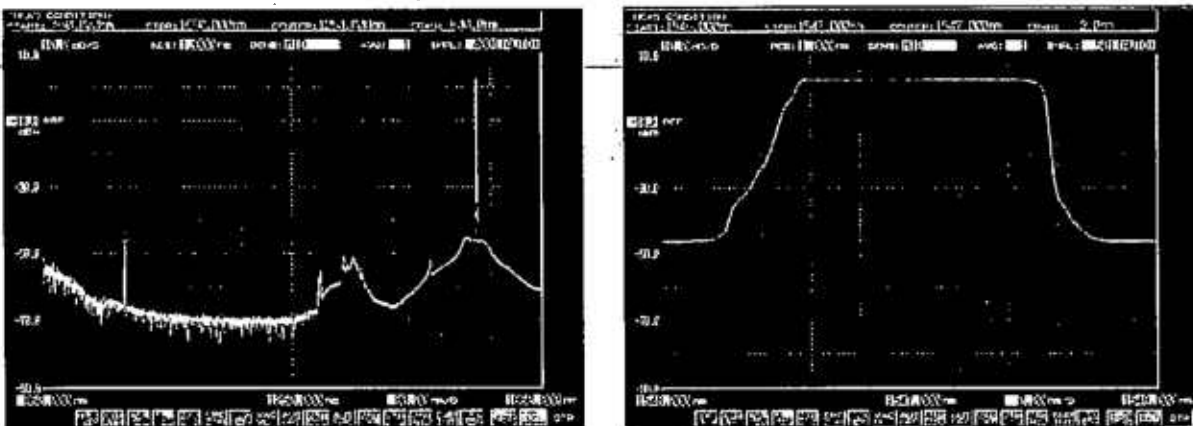


Figure 3. Left Plot: Optical spectrum of the fiber ring laser showing the pump wavelength at 980 nm and output wavelength at 1546 nm. Right Plot: Optical spectrum showing the detail of the output wavelength. Lasing is occurring over a 1 nm bandwidth defined by the fiber Bragg grating.

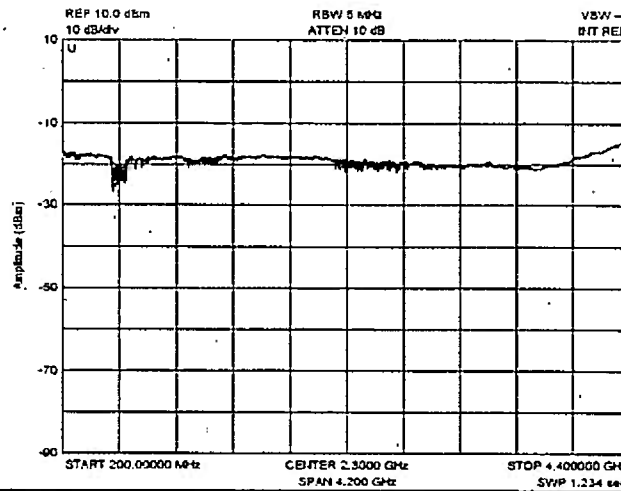


Figure 4. RF spectrum of the photo-detected output of the 1543nm fiber ring laser. The broad RF bandwidth is a result of the multiple longitudinal lasing modes.

Detail of the lasing modes can be seen in Figure 5a while the temporal response and autocorrelation of the laser output can be seen in Figures 5 b-d.

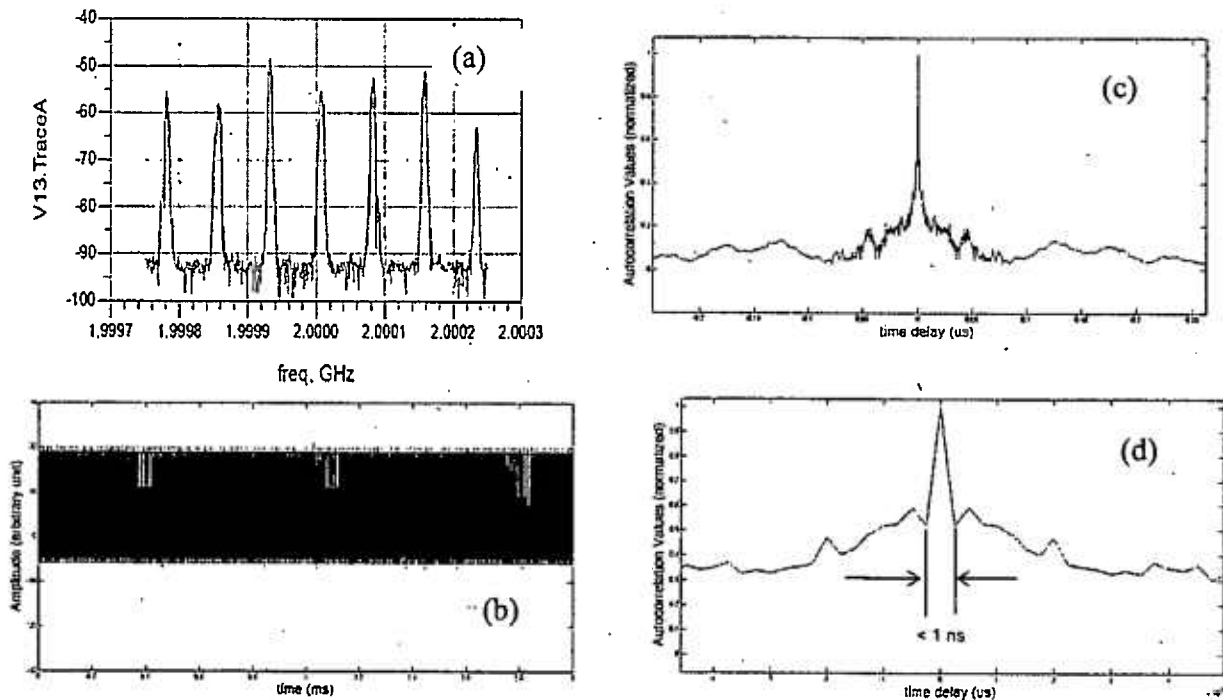


Figure 5. (a) shows simultaneous lasing of multiple modes in the 1543nm fiber ring laser which produce the noise-like temporal output of (b). The autocorrelation of (b) shows a strong autocorrelation peak in (c) which is examined in more detail in (d)

This performance is a significant accomplishment towards obtaining a broadband laser output which will allow us to investigate the laser dynamics and to explore the system-level issues of Task 2.

1071 nm Fiber Ring Laser

A 1071 nm fiber ring laser has also been developed. This wavelength is of interest since commercial fiber amplifiers and frequency doublers may be used to obtain a frequency doubled output at 536nm which is a wavelength of interest for underwater lidar. This laser uses a ytterbium (Yb) doped fiber in the gain section. The optical spectrum and temporal and autocorrelation results are shown in Figure 6. The autocorrelation results appear to be slightly better than those obtained with the 1550 nm laser; perhaps because the fiber Bragg grating has not yet been introduced and the bandwidth of the laser may be wider. This is currently being investigated in more detail. As previously noted, this laser has been developed subsequent to the August 3rd project review and additional characterization is in progress. Part of the work plan for 2012 will be to amplify and frequency double the output of this laser to support in water experiments that are planned for Task 2.

Summary of Task 3 FY11 results – The drawbacks associated with the OOR approach were fortuitous in that we accelerated our investigation into the development of wideband fiber ring lasers. We are achieving wideband lasing waveforms that exhibit excellent autocorrelation properties. Once we amplify and frequency double the 1071 nm fiber ring laser we should have a wavelength and power level suitable for underwater work. We believe that this can be done using commercially available components and will leverage similar doubling efforts being pursued by NAWC. The bandwidth of these lasers easily several GHz. This will allow the investigation into the basic science of underwater scattering at frequencies that yet to be fully explored. The issue of whether or not the laser output is chaotic or noise-like may be a moot point from the system point of view – either may provide the desired performance. However, it is an interesting open issue that will be explored in more detail in FY12.

Task 2 System Level Investigations – The ultimate goal of the wideband laser development is to use them to explore underwater optical transmission and scattering characteristics at frequencies that have yet to be fully explored. Ultimately this will determine whether or not these wide bandwidth lidar sources produce better range accuracy, resolution, and imaging capability than traditional hybrid lidar approaches. Ideally, our laser technology and system level approaches should not preclude practical system implementation due to complexity and/or cost. Therefore, our Task 2 efforts for FY11 have focused on the identification of a way(s) to process the wideband lidar signals in a practical and cost effective manner.

Several signal processing approaches that we have explored were discussed at the August 3rd project review. Approaches that were presented include several autocorrelation-based approaches, a wideband phase bridge, and a coherent noise detection approach. The autocorrelation based approach for a ranging or imaging application is shown in Figure 7. Figure 7a shows an analog based approach while figure 6b shows a digital signal processing approach.

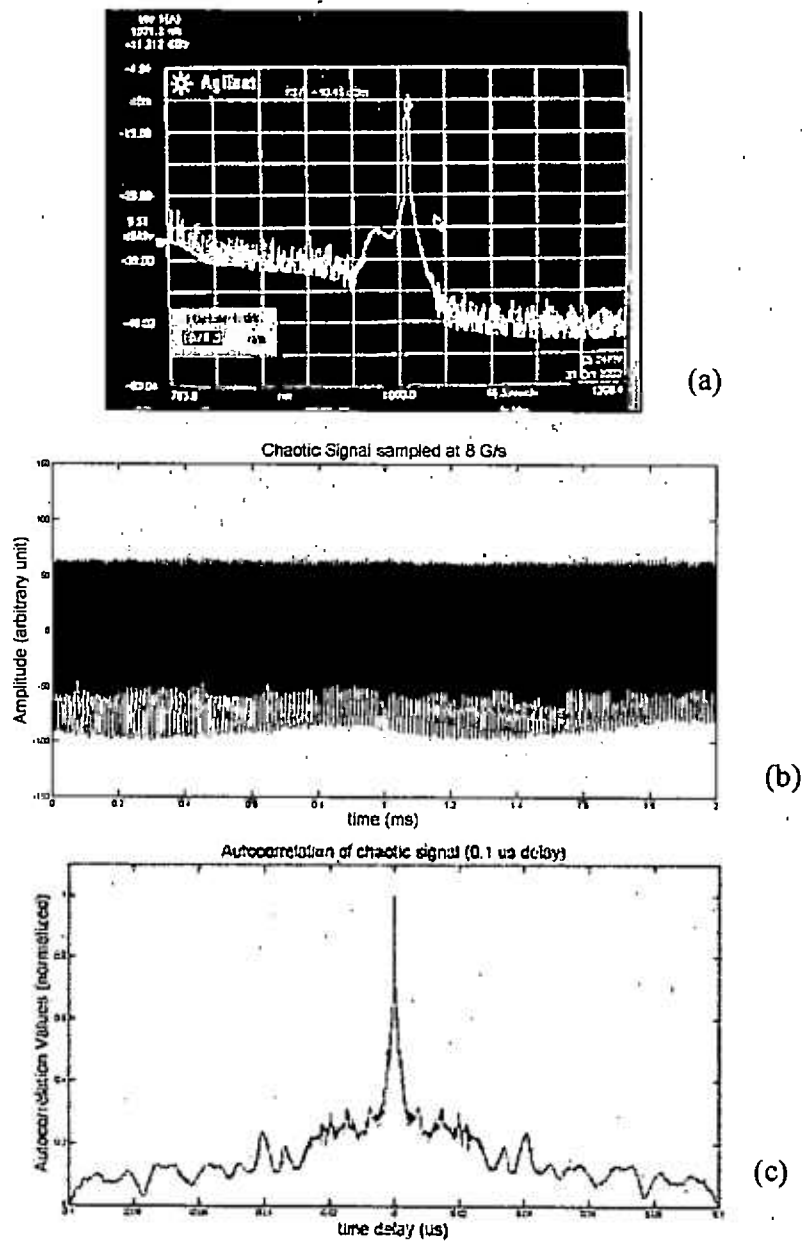


Figure 6. (a) optical spectrum of the 1071 nm fiber ring laser (b). temporal output of the fiber ring laser sampled at 8 G/s (c) autocorrelation of the output of (b) showing a strong autocorrelation peak

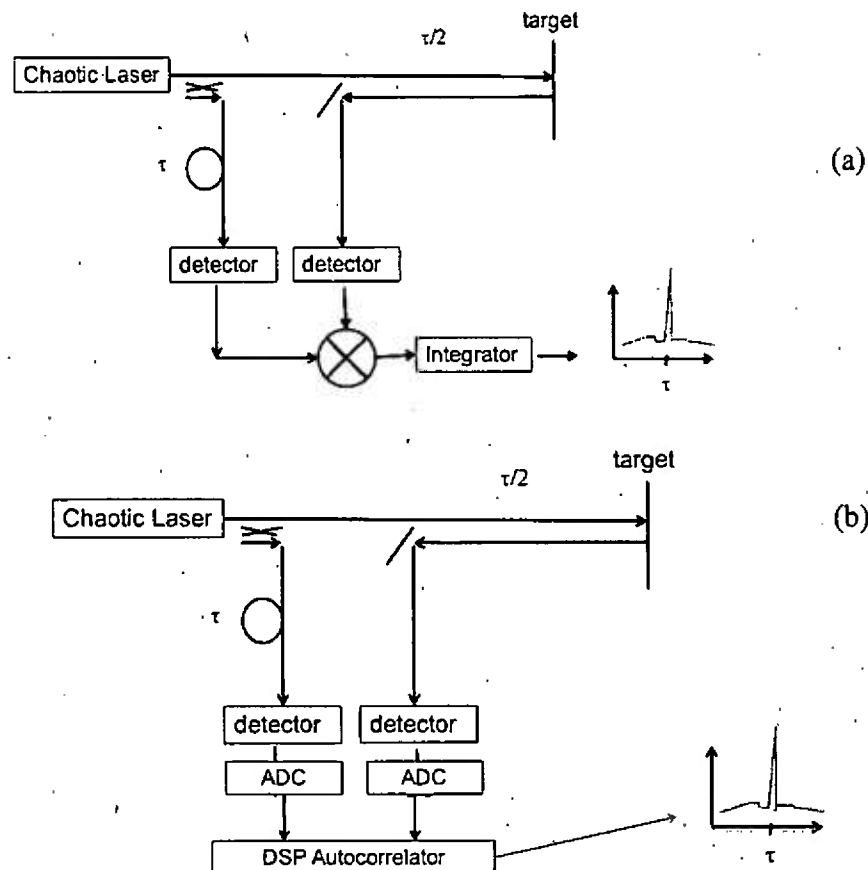


Figure 7. (a) autocorrelation signal processing approach based on analog techniques; (b) autocorrelation approach based on digital signal processing techniques

The use of a dual channel high-speed digitizer, as shown in figure 7b can be used to achieve wideband autocorrelation. In fact, it is the approach that has been used to obtain the experimental autocorrelation results described in Task 3. LeCroy and other companies make this type of test equipment with digitization rates in the 2-50 Gb/s. While this approach has advantages for laboratory work, it is not desired for system implementation due to the cost of the equipment. A 6 Gb/s digitizer is currently priced at approximately 25K.

We explored a variation of the approach shown in figure 7b. In this variation, the ADC sample rate is chosen well below the Nyquist frequency. Normally this would produce undesired aliasing effects in the digital representation of the signal. However, for a ranging application we are not interested in the

signal reconstruction, but rather the signal autocorrelation. Our simulations showed that we could sample well below the Nyquist rate without degrading the width of the autocorrelation peak (which is a measure of range) as long as the delay, τ , shown in Figure 7 is adjusted prior to digitization. The advantage to lowering the sampling rate is that cheaper digitizers may be used and there is less data to process. The tradeoff is a decrease in the level of the autocorrelation peak to the range (time) sidelobe level. Figure 8 shows that the autocorrelation peak width (lower trace) stays constant as the sampling rate is decreased. For example, an 8Gb/s sampling rate could be reduced by a factor of 256 to 31 MHz while still maintaining a 10 dB autocorrelation peak to time sidelobe level.

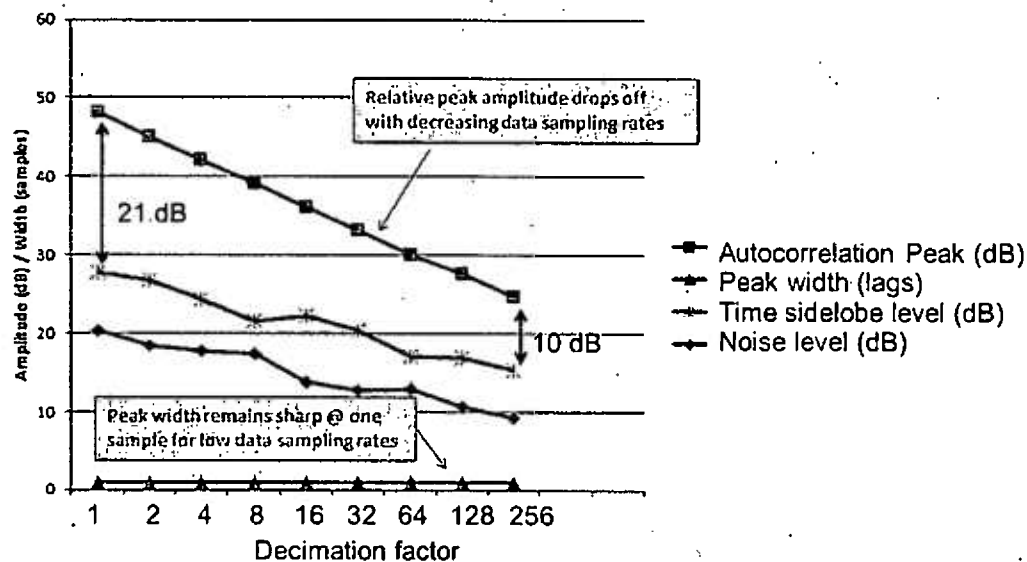


Figure 8. Simulation result showing that range accuracy is maintained as sampling rate is lowered (decimation factor is increased) if τ is adjusted prior to digitization. The autocorrelation peak to time sidelobe level is reduced, however.

A second approach that we have analyzed is a coherent noise detection scheme shown in Figure 9a. This approach has been used for noise radar and it is a physical embodiment of the Wiener-Khinchin theorem which allows the autocorrelation to be written in frequency domain quantities. In this approach the lidar output is delayed and then mixed with an intermediate frequency to form a reference signal. The lidar return is then mixed with this reference signal and all information required to form the autocorrelation maps to a single IF frequency. A low speed ADC may then be used to sample the IF to generate the autocorrelation peak. This process was simulated for a signal with a 1 GHz bandwidth. These results are shown in Figure 9b. Various decimation rates were also used in the simulation in a manner previously described. We believe that this is a promising approach and we are currently in the process of building hardware to validate the technique experimentally using our 1550nm fiber ring laser in free space.

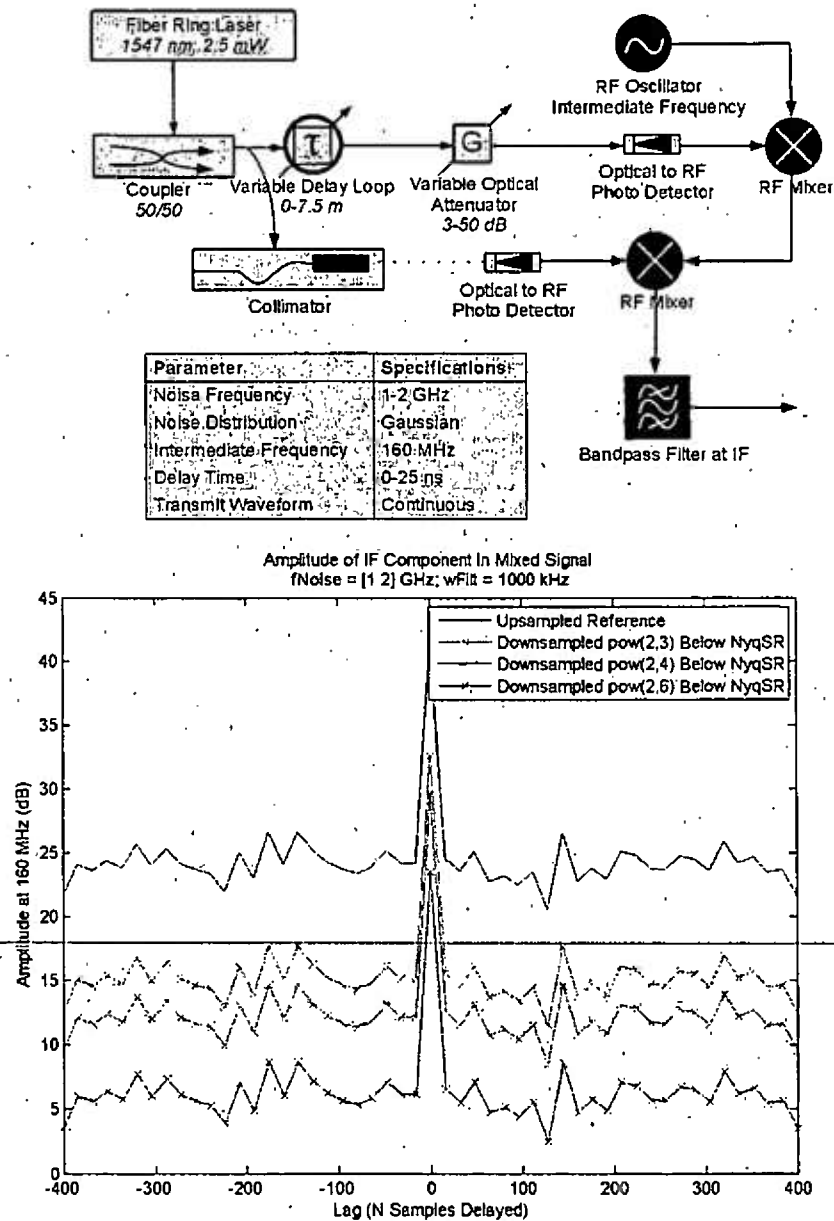


Figure 9. a) Coherent noise detection scheme; b) Simulation result showing range accuracy is maintained as sampling rate is lowered (decimation is increased) if τ is adjusted prior to digitization. The autocorrelation peak to time sidelobe level is reduced, however.

Summary – We have made significant progress towards the development of a wideband laser that will have an appropriate wavelength and power level for underwater lidar experiments. We believe that the bandwidth of these lasers will allow the underwater scattering properties to be explored at frequencies that have received little experimental attention to date. We have identified a promising approach for processing range information from the lidar signal and an experimental validation of this approach in free space is currently in progress.

Budget and Schedule:

The PI did not receive authorization to begin working on the project from the Clarkson Division of Research until November 11th, 2010. This delayed the recruitment of a Ph.D. student. Mr. Luke Rumbaugh joined the project on June 15th 2011. Mr. Rumbaugh is a Ph.D. student at Clarkson University. The project is now staffed as originally planned.

Clarkson submitted its first invoice of \$26,284 to ONR on 3/29/2011 for the second quarter (Q2) of FY2011. A second invoice covering the third quarter of 2011 was submitted in the amount of \$28,953.07 for a total project expenditure of \$55,237 through June 30th. We anticipate that the total project expenditures through the end of the government fiscal year (Sept. 30th 2011) will be approximately \$104,500.

Short Work Statement for FY2012

In FY2012 we plan to continue our work on Tasks 2 and 3. Specifically we plan the following work:

Wideband Laser Development – The 1071 Yb fiber ring laser will be optimized and fully characterized. An amplification and frequency doubling approach will be identified and implemented for this laser in order to achieve an output at 536 nm for water tank experiments. It is anticipated that commercial fiber amplifiers and frequency doublers will be used. We will also begin to explore techniques to model the fiber ring laser with the goal of being able to predict the lasing wavelength, bandwidth, and output power. This simulation will also help us to quantify the chaotic/noise properties of the laser. Methods to experimentally quantify the chaotic/noise properties will also be explored.

System Level Experiments – Signal processing approaches for range determination will continue to be explored with a primary emphasis on experimental work. These approaches will be tested in an air environment at 1550 nm to quantify their fundamental performance limits in the absence of scattering. The 536 nm laser will then be used in a water environment to explore the benefits of wideband operation in an underwater scattering environment. The sequence of experiments will closely follow those outlined in the original proposal. Specific attention will be paid to experiments that address range resolution, range accuracy, and signal to noise performance. A series of carefully controlled experiments will be conducted to assess performance in various water turbidity conditions. Initial experiments will be conducted in a small water tank at Clarkson University. Additional experiments will be conducted at NAWC Patuxent River using their large water tank facility to verify the short path length data and determine what effect longer physical path lengths have on the lidar performance.

First, the range resolution and accuracy will be determined at a finite set of optical wavelengths. The experiments will be performed in free space and then in a small water tank (e.g., a large aquarium). Maalox will be added to adjust the scattering properties of the tank water, and Nigrosin dye will be added to increase the water absorption. The exact amounts of Maalox and Nigrosin dye will be determined through collaboration with scientists at NAWC Patuxent River who have made extensive measurements of these substances in water. This will allow the performance to be measured as a function of turbidity.